Materials Transactions, Vol. 60, No. 8 (2019) pp. 1411 to 1415
Special Issue on Recent Advances in Indentation Technique

Nano-Indentation Measurement for Heat Resistant Alloys at Elevated Temperatures in Inert Atmosphere

Jovana Ruzic, Ikumu Watanabe*, Kenta Goto and Takahito Ohmura

Research Center for Structural Materials, National Institute for Materials Science, Tsukuba 305-0047, Japan

A new approach of nano-indentation measurements at elevated temperatures has been developed to evaluate a temperature-dependent mechanical behavior of heat resistant alloys on a submicron scale, where the measurement is conducted in an inert atmosphere to prevent the surface oxidation of a sample and heat an indenter passively. The developed approach enables us to perform nano-indentation testing with a diamond indenter in the temperature range of 23∼800°C. The developed approach has been applied to gamma single-phase single-crystal of a nickel-based superalloy. Then the degradations of the sample surface and the indenter tip have been discussed in this case.
[doi:10.2320/matertrans.MD201909]

(Received February 28, 2019; Accepted April 19, 2019; Published July 25, 2019)

Keywords: *high-temperature nano-indentation, hardness, elastic modulus, nickel-based superalloy*

1. Introduction

Nano-indentation measurements have been used extensively in materials research owing to its non-destructive nature, relatively simple specimen preparation, the ability to extract mechanical properties directly from load-displacement curves, etc.[1,2] Furthermore, it enables the observation and analysis of small-scale deformation, dislocation nucleation, size-dependent plasticity, phase transformation, and surface degradation at elevated temperatures.[3–7] Recently, high-temperature nano-indentation measurements have been widely employed in industries such as aerospace, automotive, nuclear, cutting tool, and biomaterials. The need for material characterization at elevated temperatures has increased toward the development of novel structural materials which can withstand challenging operating conditions, such as high temperatures.

Pioneering works on nano-indentation tests at elevated temperature was done by Poisl, *et al.*[8] and Suzuki and Ohmura.[9] Poisl, *et al.*[8] performed the indentation measurements on amorphous selenium samples up to the maximum temperature of 34°C by controlling the room temperature. Suzuki and Ohmura[9] reported the first high-temperature indentation measurements up to 600°C on silicon samples. Since 2000, the concern on measurement systems of high-temperature nano-indentation testing including systems of heating and atmosphere control has been growing. The development of commercial high-temperature nano-indentation testing systems is outlined in Table 1; products which can be mounted in scanning electron microscope and transmission electron microscope chambers are excluded from this list.

The feature and possible applications of these commercial systems were summarized in the previous studies.[10–12] There still remain several operational issues in these high-temperature nano-indentation systems: thermal stability (control of thermal equilibrium and drift), appropriate indenter selection, preventing oxidation (using vacuum or inert environment), and proper experimental design. Especially the thermal management is important to reduce the thermal drift and obtain reliable and reproducible results. There are two heating system options: active and passive. The active heating is a system to heat an indenter and a sample independently.[3,4,11] On the other hand, in the passive heating system, an indenter gains heat from a sample and atmosphere. Past studies[13,14] reported that although the passive heating provides favorable results, the passively heated indenter acts as a local heat sink, whence it is difficult to reach the equilibrium temperature between an indenter and a sample.

The material of an indenter is another concern in high-temperature nano-indentation measurements. With the objective of high elastic stiffness and high hardness at elevated temperatures, diamond, sapphire, cubic boron nitride (cBN), tungsten carbide (WC), and boron carbide (B4C) have been widely used. Despite diamond possesses the highest hardness and better thermal conductivity in comparison to the other candidates of the indenter material, it cannot be used in air at temperatures over 400°C due to the oxidation and for steel samples at temperatures over 500°C due to formation of iron carbides.[12,13] Therefore, sapphire and cBN are chosen as good substitutes because of the better chemical stability.

The present work aims to develop an approach of nano-indentation measurement to evaluate mechanical behaviors of heat resistant alloys at elevated temperatures. For this aim, the nano-indentation equipment using a high-temperature stage has been set up in a vacuum chamber, where the indenter is passively heated in an inert environment. Then we have investigated and discussed issues of the thermal management and the durability of a diamond indenter in application on a sample of a nickel-based superalloy.

2. Thermal and Atmosphere Control System in High-Temperature Nano-Indentation Measurement

For measurements at elevated temperatures, nano-indentation testing equipment using high-temperature stage (Bruker Co.) placed in a vacuum chamber on a vibration isolation stage (Minus K Technology Inc.) is used. The vacuum chamber is equipped with gas inlets allowing inner environment control and gas introduction, and with an

*Corresponding author, E-mail: WATANABE.Ikumu@nims.go.jp

Table 1 Historical development of commercially available high-temperature nano-indentation devices.

Year	Company	Operating temperature	Test environment
1994	Nano Instruments, Inc. *	-100~300°C	vacuum
2000	Micro Materials Ltd. **	up to 200°C	air
2006	Hysitron †	up to 400°C	gas
2010	Hysitron †	up to 600°C	vacuum and gas
2010	CSM Instruments SA ‡	up to 110°C	air
2011	Micro Materials Ltd. **	up to 400°C	vacuum
2011	Keysight Technologies, Inc.* / SURFACE systems+ technology GmbH & Co. KG	up to 500°C	gas
2015	Alemnis	up to 600°C	vacuum
2015	Micro Materials Ltd. **	-100~950°C	vacuum and gas
2017	Anton Paar GmbH	-150~800°C	vacuum

* In 1998 Nano Instruments, Inc. was acquired by MTS Systems Co., and sold to Agilent Technologies, Inc. in 2008. A year after, a group of experts left Agilent, Inc. and established a new company named Nanomechanics, Inc. In 2014, Agilent, Inc. split into two companies, one of which was named Keysight Technologies, Inc. In 2018, KLA-Tencor acquired Nanomechanics, Inc. and the nano-indenter product line from Keysight Technologies, Inc.
** Acquired by Spantech Products Ltd in 2017.
† Acquired by Bruker Co. in 2017.
‡ Acquired by Anton Paar GmbH in 2013.

external cooling system. The vacuum chamber is cyclically evacuated up to 1.33 mPa (10^{-5} Torr) and backfilled with argon gas (99.9999% purity) to reduce the oxygen gas level before heating.

A sample is placed between two independently-controlled heaters and heated simultaneously from the top and the bottom as illustrated in Fig. 1. The dual heating system is employed to generate a uniform temperature within the sample, in which the heating rate sets up slow (~10°C/min). Here the indenter is heated passively. At room temperature (before heating), the indenter tip is brought to 100 μm height above the sample surface and heated together with the sample, where it can be assumed that the tip is heated with almost the same heating rate as the sample. The tip and the sample are held at the predetermined temperature for 1–2 hours to achieve the thermal equilibrium between them for the thermal stabilization before the nano-indentation measurements. Heat radiation and convection are the primary sources of heat transfer during heating and thermal stabilization period. It is noted that the thermal stabilization process contributes to reduce the thermal drift in high-temperature measurements. Without this process, the measurements are failed due to the thermal drift caused by the high temperature gradient between the indenter tip and the sample. Additionally, in this study, the indenter tip is kept on the sample surface with a small force (~1 μN) for a period of 180 sec to ensure the better thermal equilibrium before each indentation.

The thermal and atmosphere control system enables us to use a diamond indenter for the following high-temperature nano-indentation measurements.

3. Application to Nickel-Based Superalloy

3.1 Sample and experimental conditions

In this study, a sample made of gamma single-phase single-crystal of a nickel-based superalloy was prepared for the measurements, which was 2 mm in height and 8 mm

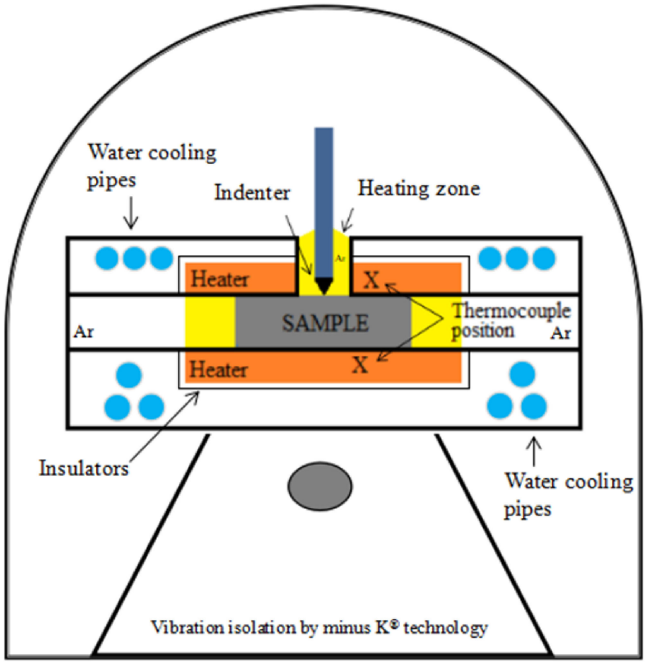

Fig. 1 Schematic view of high-temperature nano-indentation system inside vacuum chamber.

Table 2 Thermal drift rates measured by nano-indentation system.

Temperature(°C)	Thermal drift rate(nm/sec)
23	0.04±0.02
200	0.01±0.03
400	-0.06±0.08
500	0.01±0.07
600	-0.07±0.08
700	-0.03±0.11
800	-0.04±0.21

in diameter. The sample was mechanically polished, in particular, with 0.05 µm colloidal silica suspension (Master-Met, Buehler) as a final step to minimize the surface damage.

The nano-indentation measurements at elevated temperatures up to 800°C were performed using a 3,000 µN applied load with a diamond Berkovich indenter. The loading/unloading rate and the dwell time were changed in the range of 50–300 µN/sec and 10–60 sec, respectively, to investigate the creep effect in Section 3.3. The loading/unloading rate of 300 µN/sec and the dwell time of 10 sec was employed in the other sub-sections.

The thermal drift rate which is monitored by the nano-indentation system was on the order of ±0.06 nm/sec in almost all experiments and did not vary significantly with increasing temperature (Table 2). The thermal drift can be estimated from the holding segment at the maximum applied load.[11,15,16)]

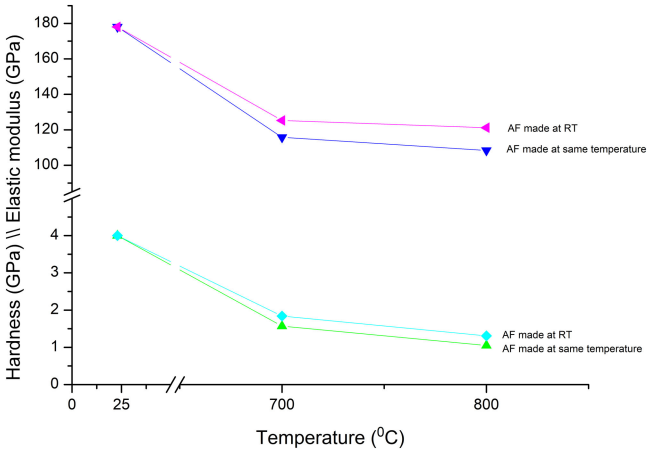

Fig. 2 Differences in calculated elastic modulus and hardness values of nickel-based superalloy sample using area function calibrated at room temperature and at the same temperatures with nano-indentation measurements.

3.2 Geometry effect of indenter tip

In the present approach, values of elastic modulus (E_r) and hardness (H) are calculated from the load-displacement curve on the basis of Oliver-Pharr method,[17)] same as a standard nano-indentation measurement at room temperature. For the sake of simplicity, the effect of pile-ups and sink-ins is not taken into account in the calculation of elastic modulus and hardness in the conventional approach. According to previous studies,[11,18)] if the thermal drift is measured to be low, it has a negligible effect on elastic modulus and hardness values which are obtained from nano-indentation measurements performed within seconds. Consequently, in the present approach, the measured elastic modulus and hardness values can be used without any additional correction.

A calibration procedure of the indenter tip is required to consider the current non-perfect geometry of the indenter tip, which is characterized by area function (AF), with a standard sample for which fused silica is used usually. The calibration can be done at room temperature before and after high-temperature measurements. In the present approach, the indenter tip is calibrated at the same temperature as the corresponding nano-indentation measurements, in which fused silica is available as the standard sample because the temperature dependency of elastic modulus and hardness is known.[18,19)] These two approaches are compared in Fig. 2, in which the values of elastic modulus and hardness with the AF calibrated at room temperature exhibit higher (about 20% higher at 800°C) than those with the AF calibrated at the same temperature as the nano-indentation measurements. It is noted that the values with the AF calibrated at the same temperature as the nano-indentation measurements show better agreement with the values in the literature.[20)] Therefore, this approach was adopted for the further data analysis in this study.

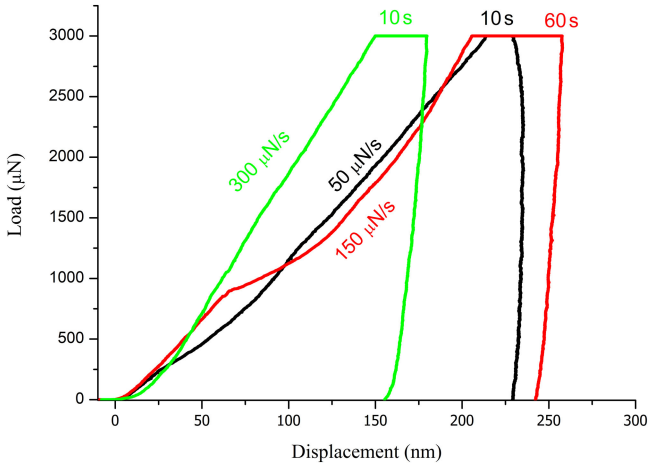

Fig. 3 Effect of loading/unloading rate and dwell period at maximum applied load at 800°C.

3.3 Creep effect

In high-temperature measurements, the effect of creep is inevitable and one of critical issues. In general, the creep becomes dominant beyond 400°C, when the negative stiffness can be observed in the unloading segment of the load-displacement curve.[21] The effect can be minimized by high loading/unloading rate and short dwell period at the maximum applied load because it is definitely a time-dependent behavior. Figure 3 shows the dependency of the loading/unloading rate and the dwell period at the maximum applied load on the load-displacement curve at 800°C. In the case of very slow loading/unloading rate (50 μN/sec), the negative stiffness can be observed at the unloading segment. Following the results in Fig. 3, we here employ the measurement condition, 300 μN/sec loading/unloading rate and dwell time of 10 sec.

3.4 Measurements at elevated temperatures

Using the above-mentioned approach, load-displacement curves, the elastic modulus and hardness of the sample were evaluated at elevated temperatures. The results are shown in Fig. 4. In both elastic modulus and hardness, a continuous decreasing trend appeared and became obvious above 400°C.

3.5 Degradation of sample surface and indenter tip

In high-temperature measurements, surface degradation by oxidation is inevitable even if the measurement is conducted in an inert or vacuum atmosphere.[7,22] Figure 5 shows the surface roughness of the sample after 3 hours of exposure to the corresponding temperature in a high purity argon atmosphere, which was measured using scanning probe microscope. The surface roughness increased above 600°C and became drastically high at 800°C. In high-temperature measurements, particular attention should be given to the surface state and an indentation should be performed at an appropriate area.

The degradation occurs not only on the sample surface but also the indenter tip. Although a tip is worn by a long-term usage even at room temperature, the degradation of the tip becomes significant in high-temperature measurements.

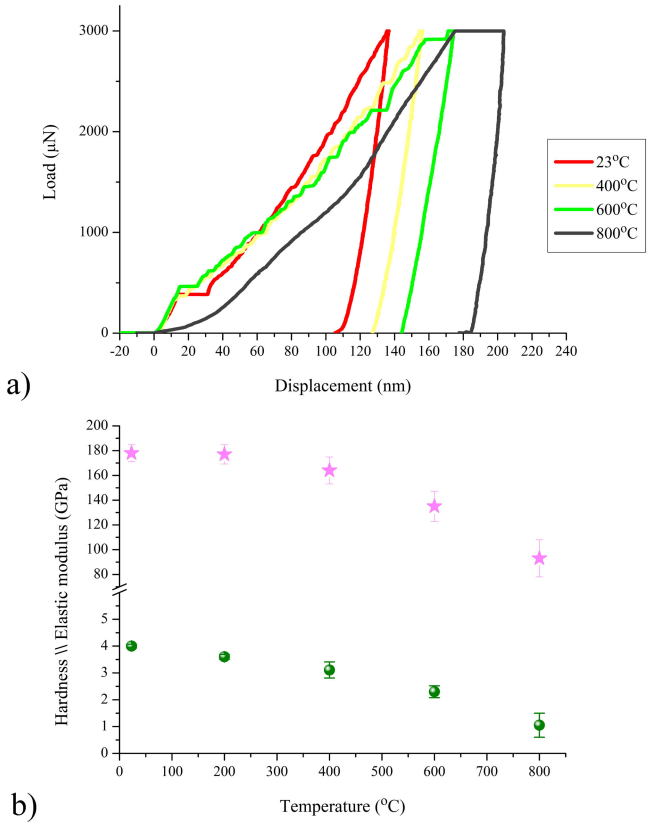

Fig. 4 Temperature-dependency of nickel-based superalloy sample at elevated temperatures up to 800°C: a) load-displacement curves and b) elastic modulus and hardness.

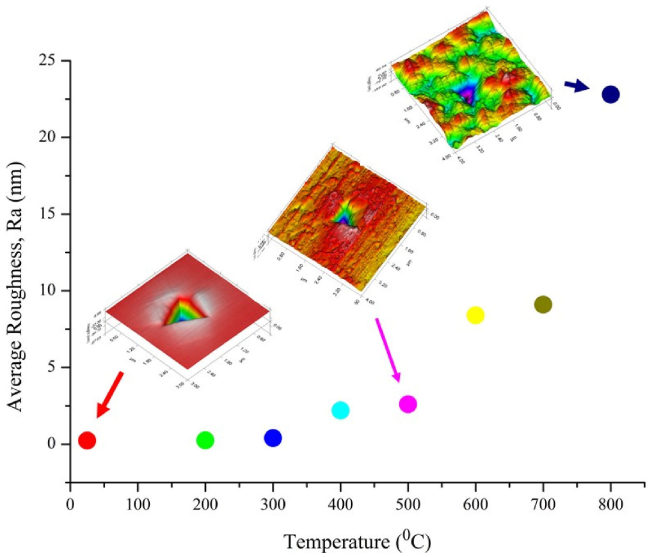

Fig. 5 Degradation of sample surface after 3 hours exposure to elevated temperature.

Figure 6 shows the comparison between an unused indenter tip and one after the usage of more than 3,000 indentations at various temperatures up to 800°C. Blunting of the indenter tip can be observed after the long-term usage. In high-temperature measurements, a chemical reaction between the indenter tip and the sample can happen, which is one of the causes for the degradation of the tip in addition to

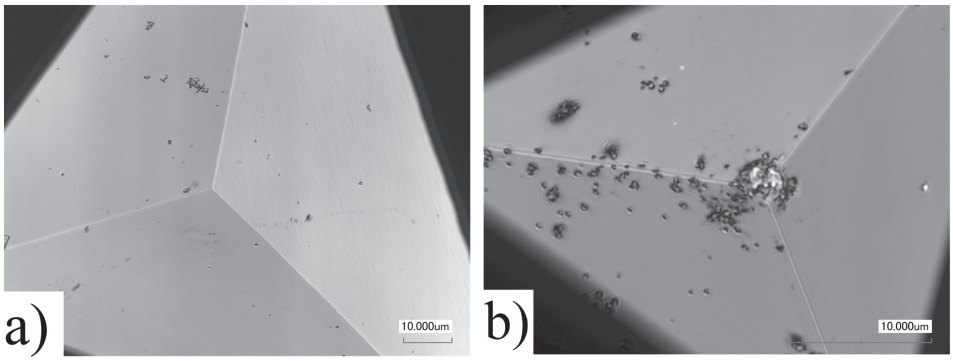

Fig. 6 Degradation of indenter tip: a) unused indenter, b) indenter after long-term usage at various temperatures up to 800°C.

the mechanical wearing. Therefore the chemical stability between materials of an indenter and a sample at elevated temperatures should be considered. Although the degradation of the indenter tip is inevitable, it can be monitored and corrected by calibrating AF at each temperature before and after a measurement.

4. Conclusion

A new approach of nano-indentation measurement at elevated temperatures up to 800°C in an inert atmosphere was developed in this study and the temperature-dependent mechanical behavior of gamma single-phase single-crystal of a nickel-based superalloy was evaluated. By passive heating and calibration of area function at each temperature, reliable measurements could be performed with a diamond indenter. The developed approach is effectual to evaluate temperature-dependent mechanical properties at a submicron scale.

The creep and the degradations of a sample and an indenter tip are essential and characteristic phenomena in the high-temperature measurements. These are key issues for further studies.

Acknowledgments

This research was financially supported by the Cross-Ministerial Strategic Innovation Promotion Program on Structural Materials for Innovation (directed by the Cabinet of Japan) and the Amada Foundation for Metal Work Technology (No. AF-2018035-C2).

REFERENCES

1) J. Ruzic, S. Emura, X. Ji and I. Watanabe: Mater. Sci. Eng. A **718** (2018) 48–55.
2) K. Goto, I. Watanabe and T. Ohmura: Int. J. Plast. **116** (2019) 81–90.
3) J.C. Trenkle, C.E. Packard and C.A. Schuh: Rev. Sci. Instrum. **81** (2010) 073901.
4) S. Korte, R.J. Stearn, J.M. Wheeler and W.J. Clegg: J. Mater. Res. **27** (2012) 167–176.
5) J.S.K.-L. Gibson, S.G. Roberts and D.E.J. Armstrong: Mater. Sci. Eng. A **625** (2015) 380–384.
6) P.S. Phani and W.C. Oliver: Acta Mater. **111** (2016) 31–38.
7) Y. Li, X. Fang, B. Xia and X. Feng: Scr. Mater. **103** (2015) 61–64.
8) W.H. Poisl, W.C. Oliver and B.D. Fabes: J. Mater. Res. **10** (1995) 2024–2032.
9) T. Suzuki and T. Ohmura: Philos. Mag. A **74** (1996) 1073–1084.
10) Z. Duan and A. Hodge: JOM **61** (2009) 32–37.
11) J.M. Wheeler, D.E.J. Armstrong, W. Heinz and R. Schwaiger: Curr. Opin. Solid State Mater. Sci. **19** (2015) 354–366.
12) S.Z. Chavoshi and S. Xu: J. Mater. Eng. Perform. **27** (2018) 3844–3858.
13) J.M. Wheeler and J. Michler: Rev. Sci. Instrum. **84** (2013) 101301.
14) N.M. Everitt, M.I. Davies and J.F. Smith: Philos. Mag. **91** (2011) 1221–1244.
15) Z. Wu, T.A. Baker, T.C. Ovaert and G.L. Niebur: J. Biomech. **44** (2011) 1066–1072.
16) J.S.K.-L. Gibson, S.G. Roberts and D.E.J. Armstrong: Mater. Sci. Eng. A **625** (2015) 380–384.
17) W.C. Oliver and G.M. Pharr: J. Mater. Res. **7** (1992) 1564–1583.
18) A.J. Harris, B.D. Beake, D.E.J. Armstrong and M.I. Davies: Exp. Mech. **57** (2017) 1115–1126.
19) M.D. Michel, F.C. Serbena and C.M. Lepienski: J. Non-Cryst. Solids **352** (2006) 3550–3555.
20) H. Takagi, M. Fujiwara and K. Kakehi: Mater. Sci. Eng. A **387–389** (2004) 348–351.
21) Y. Li, X. Fang, S. Lu, Q. Yu, G. Hou and X. Feng: Mater. Sci. Eng. A **678** (2016) 65–71.
22) X. Fang, Y. Li and X. Feng: J. Appl. Phys. **121** (2017) 125301.